


Visual Grounding with Transformers

Ye Du, Zehua Fu, Qingjie Liu , Yunhong Wang

{duyee, qingjie.liu, yhwang}@buaa.edu.cn, zuhua_fu@163.com

Abstract

In this paper, we propose a transformer based approach for visual grounding. Unlike previous proposal-and-rank frameworks that rely heavily on pretrained object detectors or proposal-free frameworks that upgrade an off-the-shelf one-stage detector by fusing textual embeddings, our approach is built on top of a transformer encoder-decoder and is independent of any pretrained detectors or word embedding models. Termed VGTR – Visual Grounding with Transformers, our approach is designed to learn semantic-discriminative visual features under the guidance of the textual description without harming their location ability. This information flow enables our VGTR to have a strong capability in capturing context-level semantics of both vision and language modalities, rendering us to aggregate accurate visual clues implied by the description to locate the interested object instance. Experiments show that our method outperforms state-of-the-art proposal-free approaches by a considerable margin on five benchmarks while maintaining fast inference speed.

1. Introduction

Visual grounding aims to locate an object instance referred by a query sentence from an image. The task has been receiving increasing attention from both academia and industry due to its great potential in vision-and-language navigation [36] and natural human-computer interaction. It can benefit many other multimodal tasks such as visual question answering [13], image caption [17] and crossmodal retrieval [29], to name a few.

Visual grounding is a challenging task. As shown in Figure 1, an object instance can be referred to by multiple referring expressions, and similar expressions may refer to distinct instances. Therefore, it requires a comprehensive understanding of both two modalities, i.e., complex language semantics and diverse image contents, not only the object instances within but also their relationships, to achieve successful visual grounding. More importantly, a model needs to establish context-level semantic correspondences across the two modalities, since the target object is distinguished

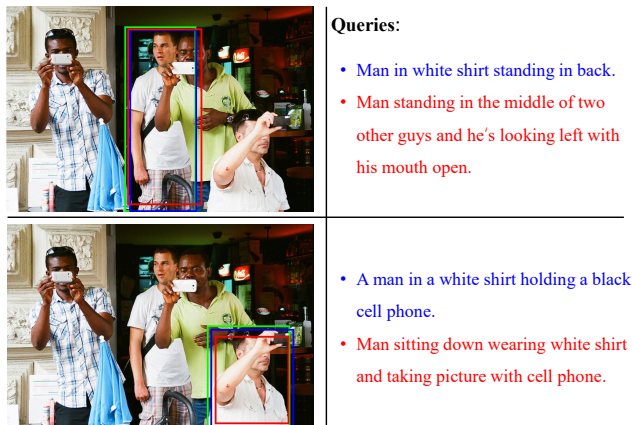


Figure 1. Illustration of visual grounding task. It is very challenging, as an object instance may be referred to by multiple query sentences, and similar expressions may refer to distinct instances. Our method is able to locate the referred instances accurately even for complex expressions. Green boxes are ground truth; blue and red boxes are results of our method. Correspondences across boxes and expressions are identified by their color.

from other objects on the basis of its visual context (i.e. attributes and relationship with other objects) and correspondences with the semantic concepts of the textual description.

Early attempts [22, 16] view visual grounding as a special case of text-based image retrieval and frame it as a retrieval task on a set of candidate regions in a given image. They leverage off-the-shelf object detectors or proposal methods to generate a set of candidate object regions and then rank them based on their similarities with the referring expression. The top-ranked one is retrieved. These methods rely heavily on the pretrained detectors and usually ignore the visual context of the object, which limits their performance, especially when the referring expression is a long sentence containing complex descriptions of object instances.

To address such limitations, some works try to encode the visual context from all proposals [23] or the entire image [41, 9]. In their settings, features of all proposals or the entire image serve as the support context for the attended

object instance. This strategy ignores the relationship modeling among objects and tends to cause the dilemma of information redundancy, i.e., not all proposals can provide useful clues for grounding the target object. To tackle this issue, some works focus on selecting a subset of proposals and model the relationship among them to form the context features. For instance, [4, 52] pay attention to a small number of proposals with the guidance of the language description; [40, 44, 43] filter object proposals according to their spatial relationships in the image.

Although summarising the attended object with a subset of proposals enables more discriminative feature learning, these methods still struggle with semantic alignment between vision and language. Besides, many of them are capped by the quality of the candidate object proposals and incur additional computational costs of generating and processing these candidates. Recently, many works [12, 5, 33, 46, 45] turn to simplifying the visual grounding pipeline by discarding the proposal generation stage and locating the referred object directly. This new pipeline performs surgery on an object detection network and implants the feature of the referring expression to augment it. Despite the elegant architecture and inference efficiency, the features of the visual and textual contexts are independent from each other. How to learn and fuse these two features more efficiently is still an open problem.

In this work, we relieve the above issues by developing an end-to-end transformer-based grounding framework, named Visual Grounding Transformer (VGTR), which is capable of capturing text-guided visual context without generating object proposals. Our model is inspired by the recent achievements of Transformers in both natural language processing [38] and computer vision [11, 39, 20, 3, 53, 8, 27]. In contrast to the recently prevalent grounding models that are built on top of off-the-shelf detectors, we propose to restructure the encoder of the transformer to process the vision and language modalities simultaneously, with the goal of understanding the natural language description and obtaining more discriminative visual evidences to reduce semantic ambiguities.

Concretely, as shown in Figure 2, our framework is composed of four main modules: basic visual encoders for extracting visual and textual tokens, a grounding encoder for performing joint reasoning and cross-modal interactions over vision and language, a grounding decoder that takes the textual tokens as *grounding queries* and feeds the output to the subsequent head for performing prediction directly. The core of our framework is the grounding encoder with visual and textual branches, in which two self-attention mechanisms, namely, the language self-attention mechanism and the text-guided visual self-attention mechanism, are leveraged to understand the semantics of the language description and learn text-guided context-aware visual features, re-

spectively.

Our contributions are summarized as follows:

- We propose Visual Grounding Transformer (VGTR), an efficient end-to-end framework to solve the visual grounding problem. Our model is independent of pre-trained detectors such as YOLO [30] and language embedding models such as BERT [10].
- We propose to learn visual features under the guidance of the language description, enabling the model to capture visual context that is consistent with the language semantics, so as to provide more accurate clues for grounding the referred object.
- Our method outperforms state-of-the-art proposal-free approaches by a considerable margin on five visual grounding benchmarks, including Flickr30K Entities [26], RefCOCO [49], RefCOCO+ [49], RefCOCOg [22], and the recently published Cops-Ref [6].

2. Related Work

In this section, we review the literature concerning visual grounding and the most recent advances in visual transformer.

2.1. Visual Grounding

Two families of visual grounding methods are frequently studied in the community: the propose-and-rank methods (also known as two-stage methods) and the proposal-free methods (also known as one-stage methods).

The propose-and-rank methods [4, 9, 52, 40, 48, 44, 43] first generate a set of candidate object proposals from the image by leveraging off-the-shelf detectors or proposal generators, then score the candidates with respect to the language description and choose the top-ranked one. These methods are limited by the performance of the pretrained detector or proposal generator. The following rank and selection stage works only if the ground truth object is extracted properly in the first stage.

The proposal-free methods [5, 46, 33, 45] focus on localizing the referred object directly without generating candidates in advance. For example, Yang *et al.* [46] reconstruct a YOLOv3 detector [30] by fusing the textual feature into the visual feature and replace the last sigmoid layer with a softmax function to directly predict the target object. This simple yet efficient paradigm has been improved by [45], in which it is proposed to reason between image and language query in an iterative manner to reduce the grounding ambiguity step by step. The strategy is particularly useful for long query scenes. Sadhu *et al.* [33] propose a single-stage modal named ZSGNet to address the challenging problem of zero-shot visual grounding. This work achieves encouraging performance in zero-shot settings. The proposal-free

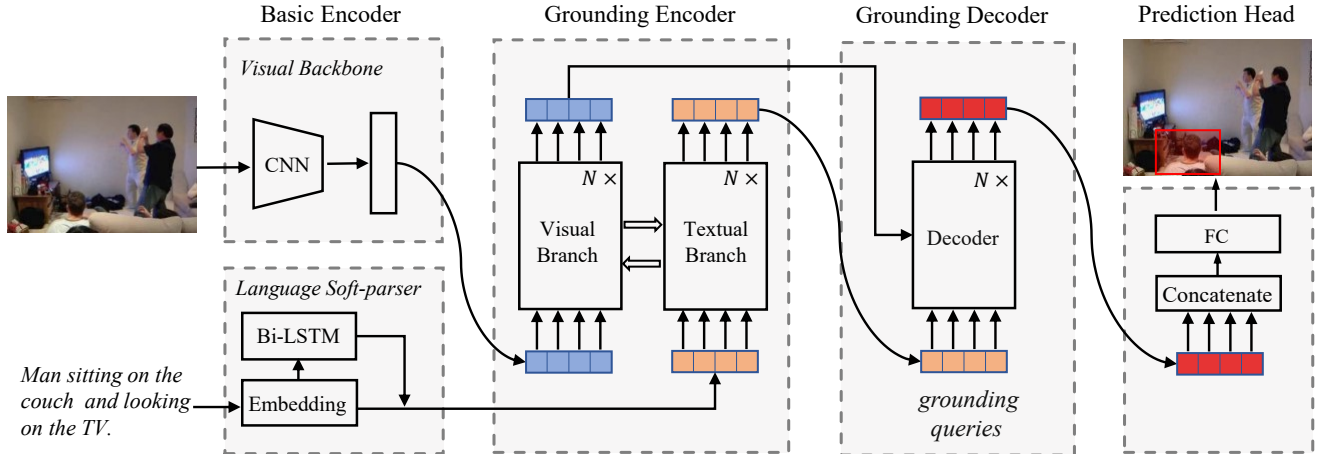


Figure 2. The overall architecture of Visual Grounding Transformer.

paradigm has shown great potential in terms of both accuracy and reference speed and is now becoming the dominant framework in the community. We refer readers to [28] for a comprehensive survey on the visual grounding task and its current solutions.

2.2. Visual Transformer

Transformer [38], originally developed for natural language processing, is a type of deep neural network based on the self-attention mechanism. Encouraged by its powerful representation ability, researchers attempt to extend this architecture for vision tasks such as object detection [3, 53, 35, 8], segmentation [39, 27], lane detection [20] and others [37]. Carion *et al.* [3] propose a new object detection framework named DETR, based on a transformer encoder-decoder architecture. Inspired by [7], Zhu *et al.* [53] introduce deformable convolution to relieve computational burden of DETR, which achieves better performance with much less training cost. Sun *et al.* [35] develop an encoder-only DETR, with improved performance but less training time. Drawn inspiration from pre-training transformers in NLP, Dai *et al.* [8] develop an unsupervised training strategy for DETR, enabling faster convergence and higher accuracy. These object detection methods reshape the image feature maps to a set of tokens and achieve comparable accuracy to state-of-the-art.

In addition to detection, other vision tasks are also enlightened by transformers. Liu *et al.* [20] use transformer to learn richer structures and context of lanes, and significantly boost the lane detection performance. Wang *et al.* [39] introduce transformer to panoptic segmentation and simplify current pipelines with a novel dual-path transformer design, which obtains outstanding performance. Tim *et al.* [27] propose an attention-based transformer to solve instance segmentation of cells in microstructures. To address multi-

modal problems in human communication, Tsai *et al.* [37] propose a multimodal transformer to align multimodal language sequences.

Inspired by these achievements, we have faith in the transformer that it may provide an excellent solution to closing semantic gaps of vision and language.

3. Approach

We introduce details of our transformer based visual grounding model in this section.

Our goal is to extract high-level and context-aware visual features under the guidance of the language expression through self-attention mechanism. To achieve this, we first use a CNN backbone to extract the relatively low-level and context-limited visual feature maps of the image and use an RNN-based soft-parser to compute a certain number of linguistic embedding vectors of the corresponding variable-length language description. Then, the visual features are transformed and reshaped to a set of visual tokens and the linguistic embedding vectors are considered as a set of textual tokens, both of which are fed into a restructured transformer encoder. The encoder processes visual and textual tokens in parallel with two distinct branches, in which a text-guided visual self-attention mechanism is introduced to learn the text-guided context-aware visual features. After the encoder step, the processed textual tokens and visual tokens are used as *grounding queries* and *encoded memories*, respectively, to be sent to a transformer decoder for regression, locating the target object directly. The overall architecture of the framework is shown in Figure 2. We will introduce each module in detail in the following subsections.

3.1. Basic Visual and Textual Encoder

Given an image and referring expression pair (I, E) , the visual grounding task aims to locate the object instance described by the referring expression with a bounding box. We first resize the whole image to $w \times h$ and forward it into a ResNet [14] architecture to extract four level features with size $\frac{w}{4} \times \frac{h}{4} \times 256$, $\frac{w}{8} \times \frac{h}{8} \times 512$, $\frac{w}{16} \times \frac{h}{16} \times 1024$ and $\frac{w}{32} \times \frac{h}{32} \times 2048$, respectively. All these features are transformed into a unified size $\frac{w}{32} \times \frac{h}{32} \times 256$, which are denoted by $[F_1, F_2, F_3, F_4]$. The final visual feature map $F \in \mathbb{R}^{\frac{w}{32} \times \frac{h}{32} \times 1024}$ is the concatenation of the transformed four level features.

$$F = [F_1, F_2, F_3, F_4] \quad (1)$$

Then, the visual feature map F is transformed and reshaped to a set of visual tokens, denoted by $X_v = \{v_i\}_{i=1}^{T_v}$, where $T_v = \frac{w}{32} \times \frac{h}{32}$ is the number of tokens, and v_i has size $d = 256$.

Instead of using complex pretrained models such as BERT [10], we propose to learn textual tokens through an RNN-based soft-parser. The architecture of our soft-parser is shown in Figure 2. For a given expression $E = \{e_t\}_{t=1}^T$, where T denotes the length of the expression, we first embed each word e_t into a vector u_t using a learnable embedding layer; then a Bi-directional LSTM (Bi-LSTM) [15] is applied to encode the context for each word and compute the attention weight on each word for each textual token q_k . The attention weight $a_{k,t}$ for the k -th textual token on the t -th word is obtained by attaching an additional full-connected (FC) layer shared by all RNN steps and a follow-up softmax function to the final hidden representation computed by the Bi-LSTM:

$$\begin{aligned} u_t &= \text{Embedding}(e_t) \\ h_t &= \text{Bi-LSTM}(u_t, h_{t-1}) \\ a_{k,t} &= \frac{\exp(f_k^T h_t)}{\sum_{i=1}^T \exp(f_k^T h_i)} \end{aligned} \quad (2)$$

Then, the weighted sum of word embeddings is used as the k -th textual token:

$$q_k = \sum_{t=1}^T a_{k,t} u_t \quad (3)$$

The final textual tokens are denoted by $X_q = \{q_k\}_{k=1}^{T_q}$, where T_q denotes the number of tokens and q_k has size $d = 256$.

3.2. Visual Grounding Transformer

To address the problem of lacking context information of the tokens obtained by the basic encoder, we propose a

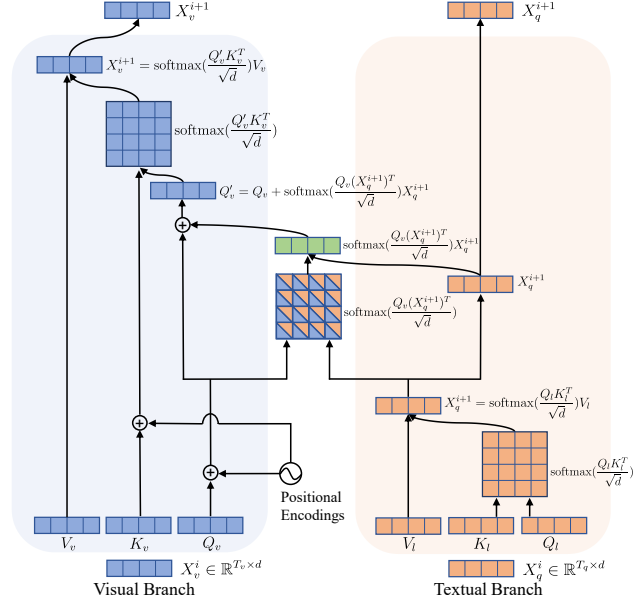


Figure 3. Detailed architecture of the visual branch, textual branch and their interactions in the grounding encoder. The norm sub-layer and FFN sub-layer are not shown here for brevity.

visual grounding transformer to further process the basic visual and textual tokens. As shown in Figure 2, our transformer consists of a two-branch grounding encoder and a grounding decoder. At below, we will introduce each module in detail.

Grounding Encoder. The grounding encoder is composed of a stack of N identical layers, where each layer has two independent branches: a visual and a textual branch, which are used to process the visual and textual tokens, respectively. This is quite different from previous works applying independent feature extraction and then fusion. Each branch consists of three sub-layers: a norm sub-layer, a multi-head self-attention sub-layer and a fully connected feed-forward sub-layer, following the design principle of keeping the original structure of the transformer as much as possible. We use pre-normalization instead of post-normalization following Xiong *et al.* [42].

As shown in Figure 3, we denote the visual Queries by Q_v , Keys by K_v , Values by V_v for the visual branch’s self-attention sub-layer, and denote the textual Queries by Q_l , Keys by K_l , Values by V_l for the textual branch’s self-attention sub-layer. Note that the visual self-attention architecture is permutation-invariant, so we supplement it with fixed positional encodings [24, 2] that are added to the visual Queries and Keys. We do not add additional positional encodings to the textual branch, because each textual token refers to a specific aspect of the text description, including the location information. After normalizing all visual and textual tokens, a standard self-attention mechanism is ap-

plied to the textual tokens:

$$\begin{aligned} Q_l &= K_l = V_l = \text{norm}(X_q^i) \\ X_q^{i+1} &= \text{softmax}\left(\frac{Q_l K_l^T}{\sqrt{d}}\right) V_l \end{aligned} \quad (4)$$

where $X_q^i = \{q_k^i\} \in \mathbb{R}^{T_q \times d}$ denotes the textual tokens that are fed into the i -th layer of the grounding encoder and $\text{norm}(\cdot)$ denotes the layer normalization operation [1]. We do not show the linear transformation, activation, dropout and shortcut connections in the formula for brevity. Instead of directly applying a separate self-attention mechanism to the normalized visual tokens, the visual Querys Q_v is then supplemented with the token-specific weighted sum of the processed textual tokens X_q^{i+1} :

$$\begin{aligned} Q_v &= K_v = \text{norm}(X_v^i) + \text{PosEncoding}(X_v^i) \\ V_v &= \text{norm}(X_v^i) \\ A_i &= \text{softmax}\left(\frac{Q_v (X_q^{i+1})^T}{\sqrt{d}}\right) \\ Q'_v &= Q_v + A_i X_q^{i+1} \end{aligned} \quad (5)$$

where $X_v^i = \{v_i^i\} \in \mathbb{R}^{T_v \times d}$ denotes the visual tokens input to the i -th layer, $\text{PosEncoding}(\cdot)$ denotes the function to obtain positional encodings, and A_i denotes the cross-modal attention matrix of the i -th layer.

Then, the text information supplemented visual Querys Q'_v , together with visual Keys and Values are used as input to another self-attention mechanism to update the visual tokens, which captures the text-guided context information essential to the visual grounding task:

$$X_v^{i+1} = \text{softmax}\left(\frac{Q'_v K_v^T}{\sqrt{d}}\right) V_v \quad (6)$$

Finally, two branch-specific fully-connected feed-forward networks, denoted by $\text{FFN}(\cdot)$, are applied to the current visual and textual tokens:

$$\begin{aligned} X_v^{i+1} &= \text{FFN}(X_v^{i+1}) \\ X_q^{i+1} &= \text{FFN}(X_q^{i+1}) \end{aligned} \quad (7)$$

Grounding Decoder. Similar to the encoder, the decoder is also composed of a stack of N identical layers. Through the encoder, we get the modified visual and textual tokens, which take the visual contexts and relevancy between two modalities into account. Then, the grounding decoder takes as input the modified textual tokens, which serve as grounding queries, and additionally attends to the modified visual tokens. In this way, we decode the text-guided visual features under the guidance of grounding queries, with the help of multi-head self-attention and encoder-decoder attention over all tokens of two modalities.

The decoder follows the standard architecture of the transformer, consisting of four sub-layers: a norm sub-layer, a self-attention sub-layer, an encoder-decoder attention sub-layer, and a fully connected feed-forward sub-layer. The self-attention mechanism over all grounding queries is the same as Eq. (4). Furthermore, we take the processed grounding queries Q_l as Querys, the text-guided context-aware visual tokens K_v from the grounding encoder as Keys and V_v as Values, and use a multi-head encoder-decoder attention mechanism followed by a fully connected feed-forward network to transform K embeddings with size d :

$$Q_l = \text{FFN}\left(\text{softmax}\left(\frac{Q_l K_v^T}{\sqrt{d}}\right) V_v\right) \quad (8)$$

Prediction Head. We denote the transformed K embeddings from the grounding decoder by $P \in \mathbb{R}^{K \times d}$, where $K = T_q$ denotes the number of grounding queries and d denotes the size of a query vector. We concatenate all the transformed vectors, and then use a prediction head consisting of two fully connected layers followed by ReLU activations to regress to the center point, width and height of the target object.

3.3. Loss

We use a linear combination of the commonly-used L1 loss and the generalized IoU (GIoU) loss [31] $\mathcal{L}_{iou}(\cdot)$ as our loss function. Overall, our prediction loss is defined as

$$\text{Loss} = \lambda_{L_1} \|b - \hat{b}\|_1 + \lambda_{L_{iou}} \mathcal{L}_{iou}(b, \hat{b}) \quad (9)$$

where b denotes the bounding box of the predicted object, \hat{b} denotes its ground truth, and $\lambda_{L_{iou}}, \lambda_{L_1} \in \mathbb{R}$ are hyper-parameters to weigh the two type of losses. Since we make prediction directly, it is simple and fast during inference.

4. Experiments

4.1. Datasets

We evaluate our model VGTR on five public benchmarks and compare it with state-of-the-art models.

Flickr30k Entities. Flickr30k Entities [26] is a phrase localization dataset that has 31,783 images with 427k referred entities. We follow the same split used in previous works [45, 25], i.e. splitting 427,193/14,433/14,481 phrases for train/validation/test, respectively.

RefCOCO/RefCOCO+/RefCOCOg. RefCOCO [49], RefCOCO+ [49], and RefCOCOg [22] are three visual grounding datasets with images selected from MSCOCO [19]. RefCOCO has 19,994 images with 142,210 referring expressions for 50,000 referred entities. RefCOCO+ has 19,992 images with 141,564 referring expressions for 49,856 referred entities. RefCOCOg has 25,799 images with 95,010 referring expressions for 49,822 referred entities. We follow the

Table 1. Phrase grounding results on Flickr30K Entities [26]. The best result is marked in bold. SS indicates Selective Search.

Method	R-Candidates	Visual Feature		Phrase Encoding	Precision	Time (ms)
		Backbone	Pretrained Detector			
GroundR [32]	SS	VGG16	None	LSTM	47.81	-
IGOP [47]	None	Multiple Network	YOLOv2	N-hot	53.97	-
CITE [25]	Edgebox	ResNet101	Fast R-CNN	Word2vec, FV	61.33	-
DDPN [51]	Proposal Net	ResNet101	Faster R-CNN	LSTM	73.30	196
ZSGNet [33]	None	ResNet50	None	LSTM	63.39	-
FAOA [46]	None	DarkNet53	YOLOv3	LSTM	67.62	19
FAOA [46]	None	DarkNet53	YOLOv3	BERT	68.69	23
FAOA2-base [45]	None	DarkNet53	YOLOv3	BERT	69.04	26
FAOA2-large [45]	None	DarkNet53	YOLOv3	BERT	69.28	36
Ours	None	ResNet50	None	LSTM	74.10	40
Ours	None	ResNet101	None	LSTM	75.25	50

Table 2. Referring expression comprehension results on RefCOCO [49], RefCOCO+ [49], and RefCOCOg [22].

Method	Visual Feature	RefCOCO			RefCOCO+			RefCOCOg			Time (ms)
		val	testA	testB	val	testA	testB	val-g	val-u	test-u	
SLR [50]	ResNet101	69.48	73.71	64.96	55.71	60.74	48.8	-	60.21	59.63	-
MAttNet [48]	ResNet101	76.40	80.43	69.28	64.93	70.26	56.00	-	66.67	67.01	320
DGA [43]	ResNet101	-	78.42	65.53	-	69.07	51.99	-	-	63.28	341
CMRE [44]	ResNet101	-	82.53	68.58	-	75.76	57.27	-	-	67.38	-
SSG [5]	DarkNet53	-	76.51	67.50	-	62.14	49.27	47.47	58.80	-	25
FAOA [46]	DarkNet53	72.54	74.35	68.50	56.81	60.23	49.60	56.12	61.33	60.26	23
FAOA2-base [45]	DarkNet53	76.59	78.22	73.25	63.23	66.64	55.53	60.96	64.87	64.87	26
FAOA2-large [45]	DarkNet53	77.63	80.45	72.30	63.59	68.36	56.81	63.12	67.30	67.20	36
Ours	ResNet50	78.29	81.49	72.38	63.29	70.01	55.64	61.64	64.19	64.01	40
Ours	ResNet101	79.20	82.32	73.78	63.91	70.09	56.51	62.28	65.73	67.23	50

Table 3. Referring comprehension results on Cops-Ref [6]. Note that the propose-and-rank methods use ground truth proposals as object candidates.

Method	R-Candidates	Precision	Time (ms)
GroundR [32]	ground truth	75.70	-
MAttNet [48]	ground truth	77.90	-
CM-Att-Erase [21]	ground truth	80.40	-
FAOA2-base [45]	None	64.49	26
FAOA2-large [45]	None	65.32	36
Ours	None	66.73	40
Ours (ResNet101)	None	67.75	50

split [45], i.e. train/validation/testA/testB containing 120,624/10,834/5,657/5,095 expressions for RefCOCO and 120,191/10,758/5,726/4,889 expressions for RefCOCO+, respectively. We experiment with the splits of RefCOCOg-google [22] and RefCOCOg-umd [23] on RefCOCOg dataset, and refer to the splits as the val-g, val-u, and test-u in Table 2.

Cops-Ref. Cops-Ref [6] has totally 148,712 expressions and 1,307,885 objects in 75,299 images. We also

follow the same split in the previous work [6], with 119,603/16,524/12,586 expressions for train/validation/test, respectively.

4.2. Implementation Details

We keep the aspect ratio of the input image and resize the long edge to 512, and then pad the resized image to the size 512×512 with the mean pixel value. The output resolution of the basic visual encoder is 16×16 , resulting in $T_v = 256$ visual tokens. We extract $T_q = 4$ textual tokens for all experiments. To make a fair comparison, we follow the same data augmentation setting in previous works [46, 45], and apply no augmentation during inference. The AdamW [18] optimizer with an initial learning rate of $1e-4$ and a batch size of 96 is used to train our model. The learning rate decreases by 10 at the 60th epoch and again at the 90th epoch. The training stops at the 120th epoch. We use ResNet50/101 [14] as our CNN backbones, which are initialized with the weights pretrained on MSCOCO [19] following previous works [48, 46, 45]. We set $N = 2$ as the default number of layers of VGTR. We set $\lambda_{L_1} = 5$ and $\lambda_{L_{iou}} = 2$.

Following previous works [46, 45], we use the Precision

metric to evaluate our approach, where a predicted object is *true positive* if its intersection over union (IoU) with the ground-truth bounding box is greater than 0.5.

4.3. Grounding Results

We first give a quantitative analysis of visual grounding results of our approach and other competitors.

Flickr30K Entities. Table 1 reports the phrase localization results on the Flickr30K Entities dataset. The top and middle parts of the table show results of previous propose-and-rank [32, 47, 25, 51] and proposal-free [33, 46, 45] visual grounding methods, respectively. The results of our proposed method VGTR are shown in the bottom part of the table. Armed with ResNet50, our model outperforms all propose-and-rank methods by large margins. For example, comparing to the state-of-the-art proposal-free method FAOA2 [45], our model outperforms it by about 5% in accuracy. Since our method uses a simple LSTM-based soft-parsner instead of complex BERT [10] as the basic textual encoder and does not depend on pretrained object detectors, we claim our performance gains come from the grounding module rather than more parameters or stronger backbone network. Additionally, we also evaluate our method using ResNet101, which produces higher-quality features, and we observe about 1% improvement over ResNet50.

RefCOCO/RefCOCO+/RefCOCog. Table 2 reports the referring expression comprehension results on RefCOCO, RefCOCO+ and RefCOCog, with the same settings in Table 1. Comparing to the proposal-free model FAOA2 [45], our method with ResNet50 backbone outperforms its basic version on almost all validation and evaluation sets, and achieves comparable performance to its large version on these datasets. On RefCOCO [49], our method outperforms FAOA2 by about 2% and achieves comparable accuracy compared to the state-of-the-art propose-and-rank method CMRE [44]. Note that the larger version of FAOA2 fine-tunes multimodal feature maps through an additional convLSTM [34] and depends on the pretrained YOLOv3 detector [30]. Comparing to the propose-and-rank methods, our model also achieves competitive results on these datasets, as well as faster inference speed.

Cops-Ref. We also evaluate our model VGTR on the recently published Cops-Ref dataset, which is proposed to solve the data bias problem [6]. As shown in Table 3, we draw similar observation that our method exceeds the state-of-the-art proposal-free method by a considerable margin. Experiments show that our model performs better on larger datasets, due to the powerful representation ability of the transformer architecture.

4.4. Ablation Study

We then conduct ablation studies from three aspects to analyse our model.

Table 4. Ablations on RefCOCO.

Decoder	Encoder			Precision
	visual	textual	text-guided	
✓				32.75
✓	✓			75.05
✓	✓		✓	78.38
✓	✓	✓		78.02
✓	✓	✓	✓	81.49

Table 5. Comparisons with other cross-modal interaction strategies (top part) and performance of different grounding module layers (bottom part) on RefCOCO.

Method	val	testA	testB
Cross-modal attention [37]	75.19	77.12	68.56
Bilinear pooling [13]	69.10	69.98	61.06
Learned modulation [45]	72.45	73.74	62.40
Ours ($N = 1$)	68.21	69.79	57.41
Ours ($N = 2$)	78.29	81.49	72.38
Ours ($N = 3$)	78.20	80.88	72.02
Ours ($N = 4$)	77.96	80.05	73.10

Contribution of each part. As shown in Table 4, we explore the contribution and necessity of each part of the model VGTR, including the grounding decoder, the textual and visual branch in the grounding encoder, and the text-guided mechanism applied to the visual branch. The first row shows the results of directly transferring visual and textual tokens from the basic encoder to the grounding decoder for regressing to the target object. Without the grounding encoder, the grounding performance decreases dramatically. The second row shows results without the textual branch, i.e., the fixed textual tokens are used directly as grounding queries and input to the grounding decoder. Then, we use the fixed textual tokens to guide the visual context learning process, without processing the textual tokens in parallel. Results are shown in the third row. In the fourth row, we experiment from another perspective by only adding an independent textual branch to the encoder, without applying the text-guided mechanism. The last row indicates results of the full model in Section 3. These results well prove the effectiveness of processing different modalities with two branches, and also the necessity of learning text-guided context-aware visual features.

Other cross-modal interaction strategies. We compare our text-guided self-attention mechanism with other cross-model interaction methods. The results are reported in Table 5. Tsai *et al.* [37] introduce a cross-modal attention mechanism for fusing information from different modalities. They use the Querys of one modality and the Keys and Values of the other modality as input of the self-attention module, which is similar to the encoder-decoder attention in the transformer decoder. We replace our text-guided self-attention with this cross-modal attention mechanism and

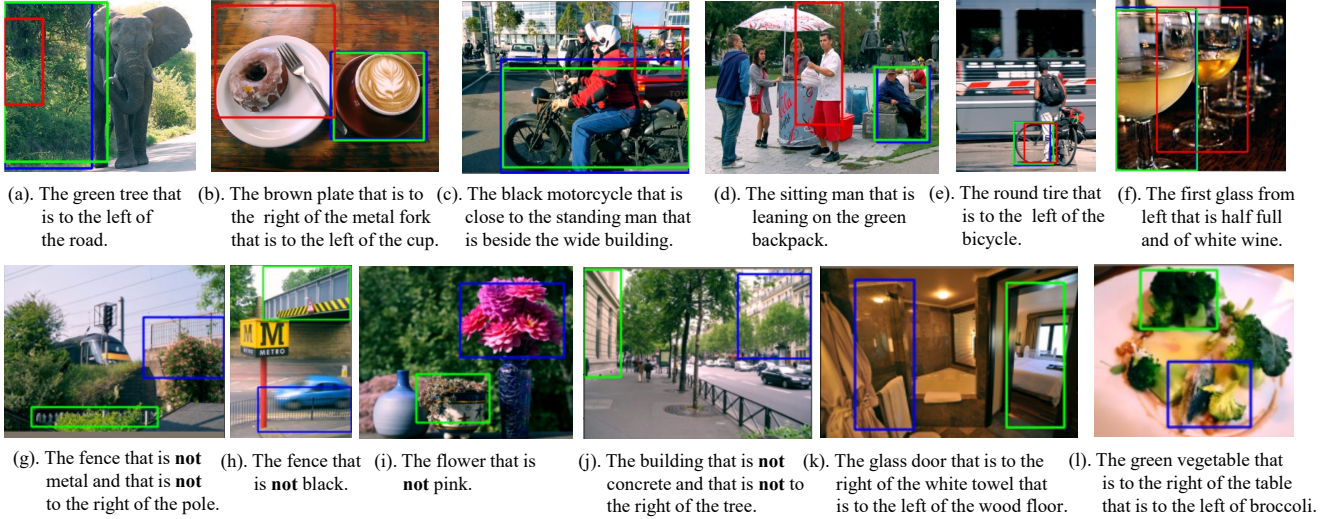


Figure 4. Challenging cases where FAOA2 [45] fails but our method succeeds (top row) and failure cases (bottom row) of our method. Blue boxes are our predictions, red boxes are FAOA2’s predictions and green boxes are ground truth.

observe about 3% drop in performance. The reason may be that the cross-modal attention mechanism continuously extracts features from the language modality and fuses it to the vision modality, which may destroy the location information in visual features. Instead, we add the weighted textual tokens to each visual Query vector to guide the visual context learning process in our method, which precludes this issue. We also explore using other methods, such as compact bilinear pooling [13] and refining the visual tokens with two modulation vectors learned from textual tokens similar to [45]. As can be observed from Table 5, the performance also drops a lot compared to our method.

Number of layers. Table 5 also presents the ablation study on the number of layers in VGTR. Experiments are conducted with the grounding encoder and decoder consisting of the same number of layers. Results show increasing the number of layers does not lead to improvements in accuracy after a dataset-specific threshold, e.g., $N \geq 2$ on RefCOCO. In order to unify the hyper-parameters over all datasets, we set $N = 2$ as the default number of layers in our experiments.

4.5. Qualitative Analysis

In the top row of Figure 4, we show some challenging cases that previous work fails but our method succeeds. It can be seen that our method performs better than previous methods in three kinds of challenging cases. The first is when grounding background stuff as opposed to things, such as the ‘tree’ in the background shown in Figure 4 (a). The second one is when language queries refer to inconspicuous objects. As shown in Figure 4 (b), the brown plate has a similar color to the table in the background, which increases difficulty of locating. The third kind is aiming at

locating the object in complex scenes and with challenging queries (Figure 4 (c)), and more accurately finding the position of the referred object (Figure 4 (e) and (f)), where our approach shows stronger discrimination and localization ability.

The bottom row shows some bad results with our method. An interesting observation is that many of the mislocalizations are generated because our model has not learnt the semantic of ‘not’, as it is a no-dementional word that may greatly expand the semantic space. Interestingly, the concept of ‘not’ is also very hard for a child learning to speak. In the cases shown in Figure 4 (g)–(j), if we remove the word ‘not’ from the query sentence, our model is able to make a self-correction and locate the referred instance correctly. Another reason for mislocalization is that some objects are difficult to be detected even for a well-trained detector, as shown in Figure 4, in which the glass door is transparent and thus hard to be identified. Semantic fuzziness of query expressions may also confuse our model to mis-locate object instances, as shown in Figure 4 (l), in which different people give different grounding results due to the ambiguity of language semantics themselves.

5. Conclusion

In the paper, we present Visual Grounding Transformer, an efficient end-to-end framework to solve the visual grounding problem. We propose to learn visual features under the guidance of the language expression. The core of our framework is the grounding encoder with visual and textual branches, capturing visual context that is consistent with the language semantics. Experiments show that our method outperforms previous grounding methods by a considerable margin.

References

- [1] Jimmy Lei Ba, Jamie Ryan Kiros, and Geoffrey E Hinton. Layer normalization. *arXiv preprint arXiv:1607.06450*, 2016.
- [2] Irwan Bello, Barret Zoph, Ashish Vaswani, Jonathon Shlens, and Quoc V Le. Attention augmented convolutional networks. In *Proceedings of the IEEE/CVF International Conference on Computer Vision*, pages 3286–3295, 2019.
- [3] Nicolas Carion, Francisco Massa, Gabriel Synnaeve, Nicolas Usunier, Alexander Kirillov, and Sergey Zagoruyko. End-to-end object detection with transformers. In *European Conference on Computer Vision*, pages 213–229. Springer, 2020.
- [4] Kan Chen, Rama Kovvuri, and Ram Nevatia. Query-guided regression network with context policy for phrase grounding. In *Proceedings of the IEEE International Conference on Computer Vision*, pages 824–832, 2017.
- [5] Xinpeng Chen, Lin Ma, Jingyuan Chen, Zequn Jie, Wei Liu, and Jiebo Luo. Real-time referring expression comprehension by single-stage grounding network. *arXiv preprint arXiv:1812.03426*, 2018.
- [6] Zhenfang Chen, Peng Wang, Lin Ma, Kwan-Yee K Wong, and Qi Wu. Cops-ref: A new dataset and task on compositional referring expression comprehension. In *Proceedings of the IEEE/CVF Conference on Computer Vision and Pattern Recognition*, pages 10086–10095, 2020.
- [7] Jifeng Dai, Haozhi Qi, Yuwen Xiong, Yi Li, Guodong Zhang, Han Hu, and Yichen Wei. Deformable convolutional networks. In *Proceedings of the IEEE international conference on computer vision*, pages 764–773, 2017.
- [8] Zhigang Dai, Bolun Cai, Yugeng Lin, and Junying Chen. Up-detr: Unsupervised pre-training for object detection with transformers. *arXiv preprint arXiv:2011.09094*, 2020.
- [9] Chaorui Deng, Qi Wu, Qingyao Wu, Fuyuan Hu, Fan Lyu, and Mingkui Tan. Visual grounding via accumulated attention. In *Proceedings of the IEEE conference on computer vision and pattern recognition*, pages 7746–7755, 2018.
- [10] Jacob Devlin, Ming-Wei Chang, Kenton Lee, and Kristina Toutanova. Bert: Pre-training of deep bidirectional transformers for language understanding. *arXiv preprint arXiv:1810.04805*, 2018.
- [11] Alexey Dosovitskiy, Lucas Beyer, Alexander Kolesnikov, Dirk Weissenborn, Xiaohua Zhai, Thomas Unterthiner, Mostafa Dehghani, Matthias Minderer, Georg Heigold, Sylvain Gelly, et al. An image is worth 16x16 words: Transformers for image recognition at scale. *arXiv preprint arXiv:2010.11929*, 2020.
- [12] Ko Endo, Masaki Aono, Eric Nichols, and Kotaro Funakoshi. An attention-based regression model for grounding textual phrases in images. In *IJCAI*, pages 3995–4001, 2017.
- [13] Akira Fukui, Dong Huk Park, Daylen Yang, Anna Rohrbach, Trevor Darrell, and Marcus Rohrbach. Multimodal compact bilinear pooling for visual question answering and visual grounding. *arXiv preprint arXiv:1606.01847*, 2016.
- [14] Kaiming He, Xiangyu Zhang, Shaoqing Ren, and Jian Sun. Deep residual learning for image recognition. In *Proceedings of the IEEE conference on computer vision and pattern recognition*, pages 770–778, 2016.
- [15] Sepp Hochreiter and Jürgen Schmidhuber. Long short-term memory. *Neural computation*, 9(8):1735–1780, 1997.
- [16] Ronghang Hu, Huazhe Xu, Marcus Rohrbach, Jiashi Feng, Kate Saenko, and Trevor Darrell. Natural language object retrieval. In *Proceedings of the IEEE Conference on Computer Vision and Pattern Recognition*, pages 4555–4564, 2016.
- [17] Andrej Karpathy and Li Fei-Fei. Deep visual-semantic alignments for generating image descriptions. In *Proceedings of the IEEE conference on computer vision and pattern recognition*, pages 3128–3137, 2015.
- [18] Diederik P Kingma and Jimmy Ba. Adam: A method for stochastic optimization. *arXiv preprint arXiv:1412.6980*, 2014.
- [19] Tsung-Yi Lin, Michael Maire, Serge Belongie, James Hays, Pietro Perona, Deva Ramanan, Piotr Dollár, and C Lawrence Zitnick. Microsoft coco: Common objects in context. In *European conference on computer vision*, pages 740–755. Springer, 2014.
- [20] Ruijin Liu, Zejian Yuan, Tie Liu, and Zhiliang Xiong. End-to-end lane shape prediction with transformers. In *Proceedings of the IEEE/CVF Winter Conference on Applications of Computer Vision*, pages 3694–3702, 2021.
- [21] Xihui Liu, Zihao Wang, Jing Shao, Xiaogang Wang, and Hongsheng Li. Improving referring expression grounding with cross-modal attention-guided erasing. In *Proceedings of the IEEE/CVF Conference on Computer Vision and Pattern Recognition*, pages 1950–1959, 2019.
- [22] Junhua Mao, Jonathan Huang, Alexander Toshev, Oana Camburu, Alan L Yuille, and Kevin Murphy. Generation and comprehension of unambiguous object descriptions. In *Proceedings of the IEEE conference on computer vision and pattern recognition*, pages 11–20, 2016.
- [23] Varun K Nagaraja, Vlad I Morariu, and Larry S Davis. Modeling context between objects for referring expression understanding. In *European Conference on Computer Vision*, pages 792–807. Springer, 2016.
- [24] Niki Parmar, Ashish Vaswani, Jakob Uszkoreit, Lukasz Kaiser, Noam Shazeer, Alexander Ku, and Dustin Tran. Image transformer. In *International Conference on Machine Learning*, pages 4055–4064. PMLR, 2018.
- [25] Bryan A Plummer, Paige Kordas, M Hadi Kiapour, Shuai Zheng, Robinson Piramuthu, and Svetlana Lazebnik. Conditional image-text embedding networks. In *Proceedings of the European Conference on Computer Vision (ECCV)*, pages 249–264, 2018.
- [26] Bryan A Plummer, Liwei Wang, Chris M Cervantes, Juan C Caicedo, Julia Hockenmaier, and Svetlana Lazebnik. Flickr30k entities: Collecting region-to-phrase correspondences for richer image-to-sentence models. In *Proceedings of the IEEE international conference on computer vision*, pages 2641–2649, 2015.
- [27] Tim Prangemeier, Christoph Reich, and Heinz Koepl. Attention-based transformers for instance segmentation of cells in microstructures. In *2020 IEEE International Conference on Bioinformatics and Biomedicine (BIBM)*, pages 700–707. IEEE, 2020.

- [28] Yanyuan Qiao, Chaorui Deng, and Qi Wu. Referring expression comprehension: A survey of methods and datasets. *IEEE Transactions on Multimedia*, 2020.
- [29] Filip Radenović, Giorgos Tolias, and Ondřej Chum. Cnn image retrieval learns from bow: Unsupervised fine-tuning with hard examples. In *European conference on computer vision*, pages 3–20. Springer, 2016.
- [30] Joseph Redmon and Ali Farhadi. Yolov3: An incremental improvement. *arXiv preprint arXiv:1804.02767*, 2018.
- [31] Hamid Rezaatoughi, Nathan Tsoi, JunYoung Gwak, Amir Sadeghian, Ian Reid, and Silvio Savarese. Generalized intersection over union: A metric and a loss for bounding box regression. In *Proceedings of the IEEE/CVF Conference on Computer Vision and Pattern Recognition*, pages 658–666, 2019.
- [32] Anna Rohrbach, Marcus Rohrbach, Ronghang Hu, Trevor Darrell, and Bernt Schiele. Grounding of textual phrases in images by reconstruction. In *European Conference on Computer Vision*, pages 817–834. Springer, 2016.
- [33] Arka Sadhu, Kan Chen, and Ram Nevatia. Zero-shot grounding of objects from natural language queries. In *Proceedings of the IEEE/CVF International Conference on Computer Vision*, pages 4694–4703, 2019.
- [34] Xingjian Shi, Zhourong Chen, Hao Wang, Dit-Yan Yeung, Wai-Kin Wong, and Wang-chun Woo. Convolutional lstm network: A machine learning approach for precipitation nowcasting. *arXiv preprint arXiv:1506.04214*, 2015.
- [35] Zhiqing Sun, Shengcao Cao, Yiming Yang, and Kris Kitani. Rethinking transformer-based set prediction for object detection. *arXiv preprint arXiv:2011.10881*, 2020.
- [36] Jesse Thomason, Jivko Sinapov, and Raymond Mooney. Guiding interaction behaviors for multi-modal grounded language learning. In *Proceedings of the First Workshop on Language Grounding for Robotics*, pages 20–24, 2017.
- [37] Yao-Hung Hubert Tsai, Shaojie Bai, Paul Pu Liang, J Zico Kolter, Louis-Philippe Morency, and Ruslan Salakhutdinov. Multimodal transformer for unaligned multimodal language sequences. In *Proceedings of the conference. Association for Computational Linguistics. Meeting*, volume 2019, page 6558. NIH Public Access, 2019.
- [38] Ashish Vaswani, Noam Shazeer, Niki Parmar, Jakob Uszkoreit, Llion Jones, Aidan N Gomez, Lukasz Kaiser, and Illia Polosukhin. Attention is all you need. *arXiv preprint arXiv:1706.03762*, 2017.
- [39] Huiyu Wang, Yukun Zhu, Hartwig Adam, Alan Yuille, and Liang-Chieh Chen. Max-deeplab: End-to-end panoptic segmentation with mask transformers. *arXiv preprint arXiv:2012.00759*, 2020.
- [40] Peng Wang, Qi Wu, Jiewei Cao, Chunhua Shen, Lianli Gao, and Anton van den Hengel. Neighbourhood watch: Referring expression comprehension via language-guided graph attention networks. In *Proceedings of the IEEE/CVF Conference on Computer Vision and Pattern Recognition*, pages 1960–1968, 2019.
- [41] Fan Wu, Zhongwen Xu, and Yi Yang. An end-to-end approach to natural language object retrieval via context-aware deep reinforcement learning. *arXiv preprint arXiv:1703.07579*, 2017.
- [42] Ruibin Xiong, Yunchang Yang, Di He, Kai Zheng, Shuxin Zheng, Chen Xing, Huishuai Zhang, Yanyan Lan, Liwei Wang, and Tiejian Liu. On layer normalization in the transformer architecture. In *International Conference on Machine Learning*, pages 10524–10533. PMLR, 2020.
- [43] Sibe Yang, Guanbin Li, and Yizhou Yu. Dynamic graph attention for referring expression comprehension. In *Proceedings of the IEEE/CVF International Conference on Computer Vision*, pages 4644–4653, 2019.
- [44] Sibe Yang, Guanbin Li, and Yizhou Yu. Relationship-embedded representation learning for grounding referring expressions. *IEEE Transactions on Pattern Analysis and Machine Intelligence*, 2020.
- [45] Zhengyuan Yang, Tianlang Chen, Liwei Wang, and Jiebo Luo. Improving one-stage visual grounding by recursive subquery construction. In *Computer Vision – ECCV 2020*, pages 387–404. Cham, 2020. Springer International Publishing.
- [46] Zhengyuan Yang, Boqing Gong, Liwei Wang, Wenbing Huang, Dong Yu, and Jiebo Luo. A fast and accurate one-stage approach to visual grounding. In *Proceedings of the IEEE/CVF International Conference on Computer Vision*, pages 4683–4693, 2019.
- [47] Raymond A Yeh, Jinjun Xiong, Wen-Mei W Hwu, Minh N Do, and Alexander G Schwing. Interpretable and globally optimal prediction for textual grounding using image concepts. *arXiv preprint arXiv:1803.11209*, 2018.
- [48] Licheng Yu, Zhe Lin, Xiaohui Shen, Jimei Yang, Xin Lu, Mohit Bansal, and Tamara L Berg. Mattnet: Modular attention network for referring expression comprehension. In *Proceedings of the IEEE Conference on Computer Vision and Pattern Recognition*, pages 1307–1315, 2018.
- [49] Licheng Yu, Patrick Poirson, Shan Yang, Alexander C Berg, and Tamara L Berg. Modeling context in referring expressions. In *European Conference on Computer Vision*, pages 69–85. Springer, 2016.
- [50] Licheng Yu, Hao Tan, Mohit Bansal, and Tamara L Berg. A joint speaker-listener-reinforcer model for referring expressions. In *Proceedings of the IEEE Conference on Computer Vision and Pattern Recognition*, pages 7282–7290, 2017.
- [51] Zhou Yu, Jun Yu, Chenchao Xiang, Zhou Zhao, Qi Tian, and Dacheng Tao. Rethinking diversified and discriminative proposal generation for visual grounding. In *Proceedings of the Twenty-Seventh International Joint Conference on Artificial Intelligence, IJCAI-18*, pages 1114–1120, 7 2018.
- [52] Hanwang Zhang, Yulei Niu, and Shih-Fu Chang. Grounding referring expressions in images by variational context. In *Proceedings of the IEEE Conference on Computer Vision and Pattern Recognition*, pages 4158–4166, 2018.
- [53] Xizhou Zhu, Weijie Su, Lewei Lu, Bin Li, Xiaogang Wang, and Jifeng Dai. Deformable detr: Deformable transformers for end-to-end object detection. *arXiv preprint arXiv:2010.04159*, 2020.